

Transmission Spectra and Derived Imaginary Refractive Indices for Soil Samples from Globally Important Dust Generating Regions

Paper Number: A55O-1304

Mohammad R. Sadrian^{1, 2} (E-mail: msadrian@nevada.unr.edu); Wendy M. Calvin¹; Johann P. Engelbrecht²; Hans Moosmüller²

¹Department of Geological Sciences and Engineering, University of Nevada, Reno, Reno, 89557, USA

² Division of Atmospheric Sciences, Desert Research Institute (DRI), Reno, Nevada 89512, USA



Desert Research Institute



University of Nevada, Reno

Introduction- Materials

We recently conducted spectral measurements on 26 surface soil samples from globally important dust generating regions for the purpose of understanding their spectral properties relative to pure minerals (Sadrian et al., 2022). Depending on the specific mineral content, absorption properties of these samples vary strongly with wavelength and are expected to have a large impact on direct aerosol radiative forcing. We measured the long-wave infrared transmission (LWIT) for six of these samples mixed in KBr pellets. These transmission measurements were used to calculate imaginary indices of refraction (k), which are critical for estimating the radiative effect of dust in the atmosphere. Then, real indices of refraction (n) were derived from k by applying a Subtractive Kramers-Kronig (SKK) technique (Hale and Querry, 1973).

Past studies such as Di Biagio et al. (2014) and (2017), measured LWIT of dust in KBr pellets and suspended in a chamber, respectively. In contrast to our study, they applied the Lorentz dispersion theory to derive n from k . We compare n and k obtained in this study with samples from similar geographic regions determined by DB 2014 and DB 2017.

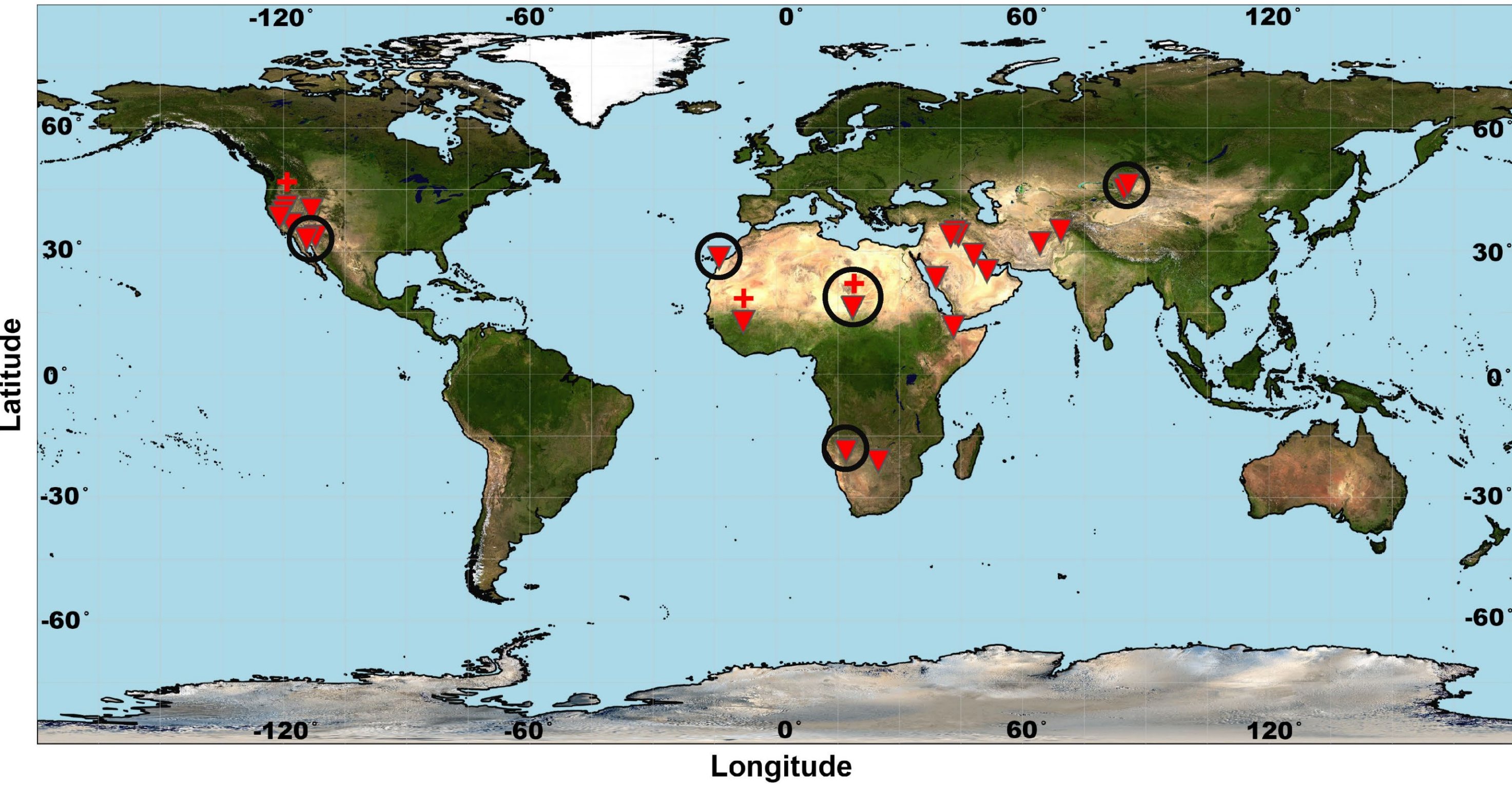


Fig1. World map with inverse triangles representing 26 soil sample locations with two representative samples used from sites marked with plus (+) (Sadrian et al., 2022). The samples shown with the black circles are used in this study.

Transmission Spectra

For this study we used soil samples that were sieved to $< 38 \mu\text{m}$ in size (Engelbrecht et al., 2016). Dust-KBr pellets were made using a mixture of 0.5 mg of soil sample with 200 mg of KBr. Measurements of long-wave infrared transmission was conducted with a benchtop Nicolet 380 Fourier Transform Infrared (FTIR) spectrometer with a wavelength range from 2.5 to 25 μm . Transmission spectra for soils show strong Si-O bonds in the $\sim 9\text{-}11 \mu\text{m}$ and $> 15 \mu\text{m}$ regions are attributed to multiple silicate minerals with overlapping absorptions. In addition, strong carbonate absorption near 7 μm likely arises from overlapping absorption features in calcite and dolomite.

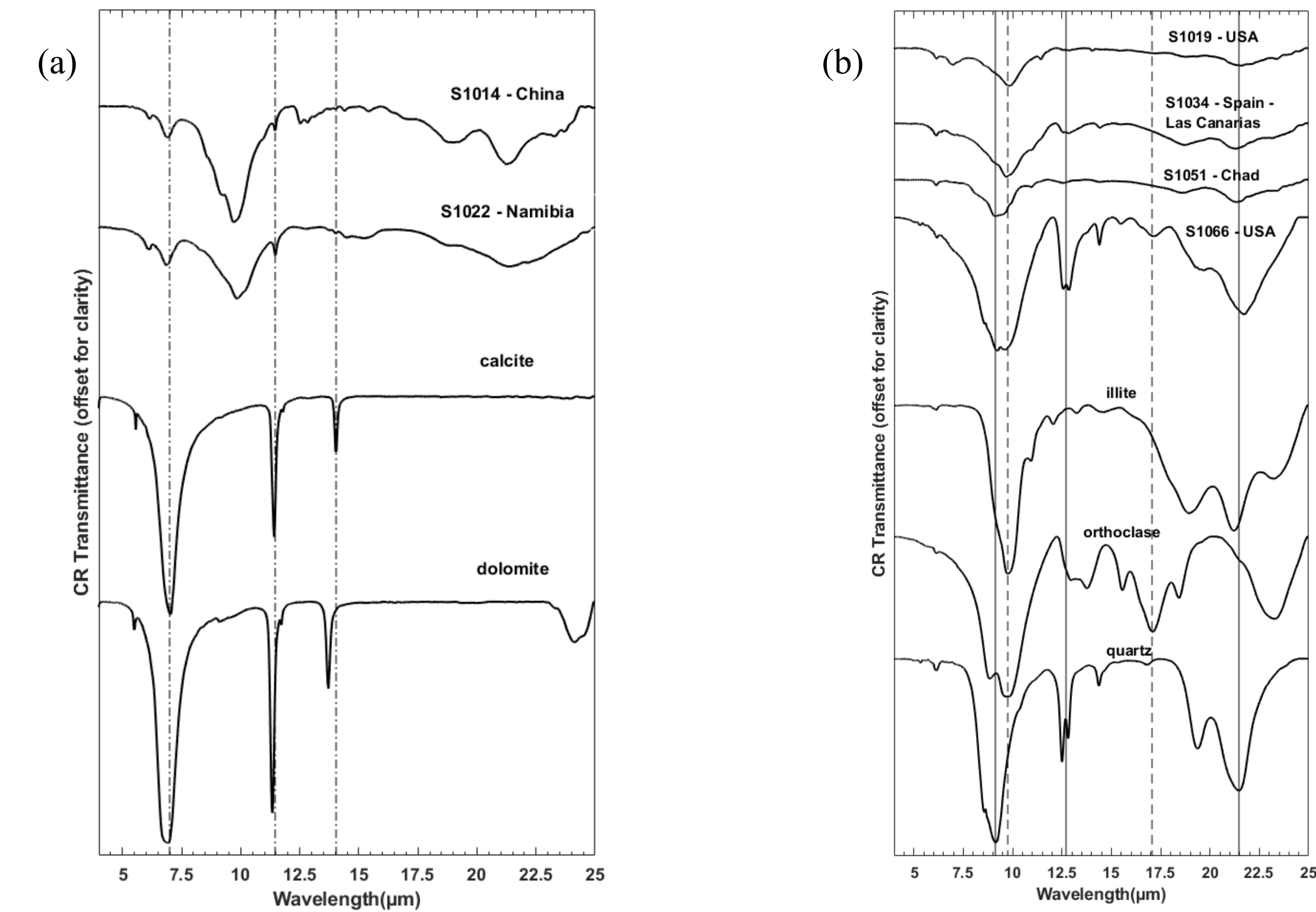


Fig 2. Figures (a) and (b) show continuum-removed transmission spectra of six representative soil samples and pure minerals from Salisbury et al., 1991. (a) Carbonate in samples is compared with calcite and dolomite absorption features. (b) Strongest silicates absorptions are compared with Si-O bonds in a few representative silicates (clay, feldspar, and quartz).

Methods

To obtain k , we first converted long-wave infrared transmission data to absorption coefficient (β_a), following Beer's law:

$$t(x) = e^{-\beta_a x}$$

where t is transmission, β_a is absorption coefficient, and x is the path length of radiation (0.57 mm thickness of the pellet) * the concentration of the dust in KBr .

Then, k was calculated using:

$$k = \beta_a * \lambda / 4\pi, \text{ where } \lambda \text{ is the wavelength.}$$

Methods-Results

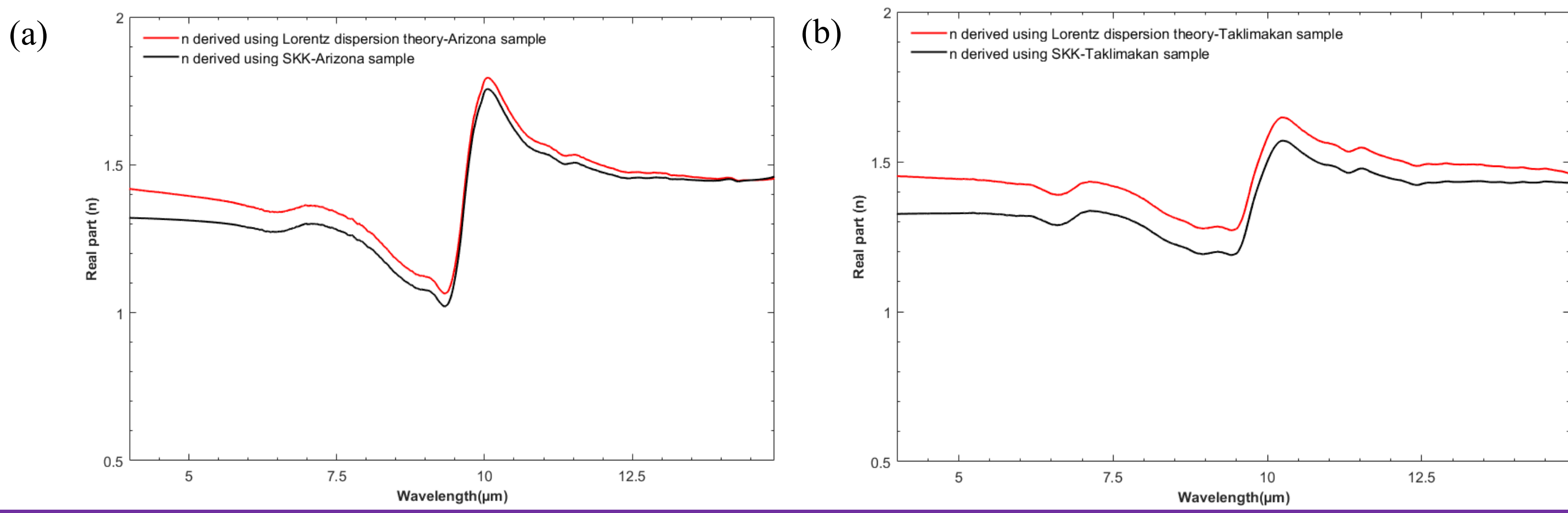
Because k is only known over a limited wavelength range, the Subtractive Kramers-Kronig (SKK) method (Hale and Querry, 1973) was used in this study to derive n from k . Past studies have successfully used SKK to derive optical constants (Dalton and Pitman, 2012; Roush, 2021). The SKK equation is as follows:

$$n(\lambda_0) = n(\lambda_1) + \text{Prin.} \left[\frac{2(\lambda_1^2 - \lambda_0^2)}{\pi} \int_0^\infty \frac{\lambda k(\lambda) d\lambda}{(\lambda_0^2 - \lambda^2)(\lambda_1^2 - \lambda^2)} \right],$$

Where $n(\lambda_1)$ is a known value for the index of refraction at wavelength λ_1 , Prin. indicates Cauchy principal value of the integral, and $k(\lambda)$ is the imaginary index of refraction at wavelength λ . We implemented the SKK method in MATLAB.

We tested the MATLAB code for SKK by determining values of n from previously published values of k from DB 2017. Figure 3 shows two samples, from Arizona and Taklimakan and compares values of n using the Lorentz dispersion theory (red line) and our SKK technique (black line). The shapes are the same and absolute values are within 10% and usually closer. Differences may be due to the method, the assumed value of $n(\lambda_1)$, or that we are only able to integrate SKK from 2.5 to 25 μm , not 0 to ∞ .

Fig 3. (a) and (b) show the n for Arizona and Taklimakan samples (DB 2017) that were derived from k using the Lorentz dispersion theory (red line) (DB 2017) and our SKK technique (black line).

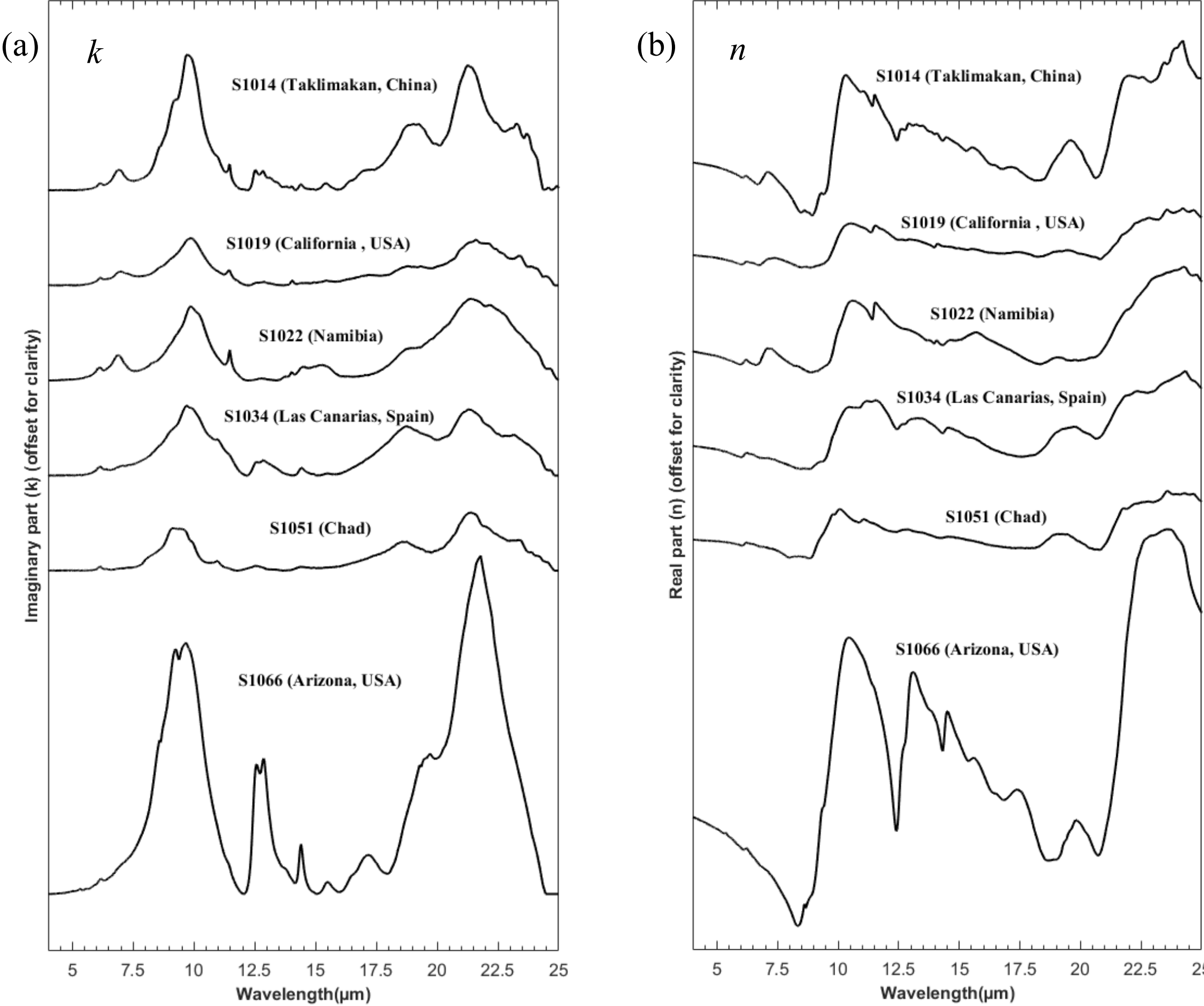


Similar to the transmission spectra, the imaginary indices (k , Fig 4a) of 6 global soil samples show mineral variability. The strong absorptions in $\sim 9\text{-}11 \mu\text{m}$ and $> 15 \mu\text{m}$ regions are not assigned to a single mineral, but caused by overlapping features of phyllosilicates, quartz, and feldspars.

The derived real indices of refraction (n , Fig 4b) for these 6 samples also show a high diversity in their spectra due to the variation in mineralogical composition.

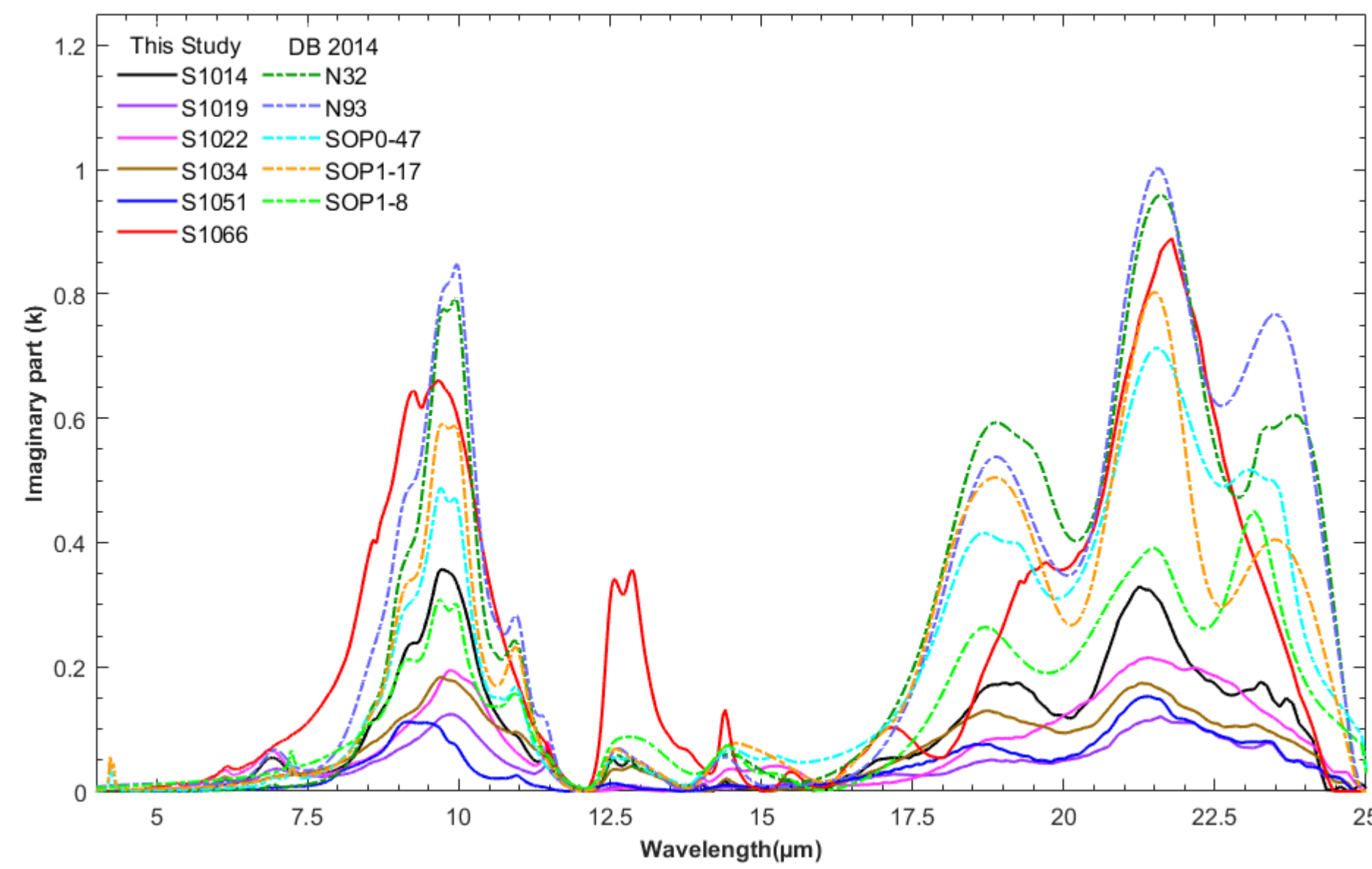
For absolute values of k and n see the plots in the Results (Fig 6).

Fig 4. (a) and (b) display k and n derived in this study. Spectra for k and n in both plots are offset for clarity.



Both this study and DB 2014 used transmission spectra of dust-KBr pellets to derive imaginary index (k). As shown in Figure 5, the k spectra from this study have greater mineral diversity, in particular between $\sim 9\text{-}11 \mu\text{m}$, compared to DB 2014. Some k spectra from this study show stronger carbonate absorption near 7 μm . Sample S1066 displays a very strong 12.5-13.5 μm quartz absorption compared to other samples. On the other hand, DB 2014 samples generally show stronger absorption peaks in the region $> 17 \mu\text{m}$.

Fig 5. k spectra obtained in this study (solid lines) are compared with ones derived in Di Biagio et al. (2014) (dot-dash lines).



Conclusion

- This study shows samples with higher mineral diversity than previous studies. This will help improve regional models of mineral dust radiative forcing.
- We note that many silicate minerals contribute to wavelengths where absorption is strongest and no sample exhibits absorption due to just one mineral.
- When compared with prior studies for samples from the same geographic location we generally see very good agreement. Except for samples from the Sahara, the magnitude of both n and k are comparable between this study and DB 2014 and DB 2017. Spectral differences can be attributed to sample diversity from the sites.
- When using the same input value of k the SKK method provides real indices that are comparable to the computationally more complicated Lorentz approach.

Results

We compare real and imaginary indices of refraction (n , k) from our study and DB 2017 for samples that are from the same geographic locations. Most samples are comparable in magnitude for both n and k . DB 2017 generally have stronger carbonate features near 7 μm . Our Arizona sample (Fig 6b) has a strong quartz absorption between 12.5-13.5 μm . Values for our study are in black in each plot. Spectral differences can be attributed to mineralogical diversity among the samples.

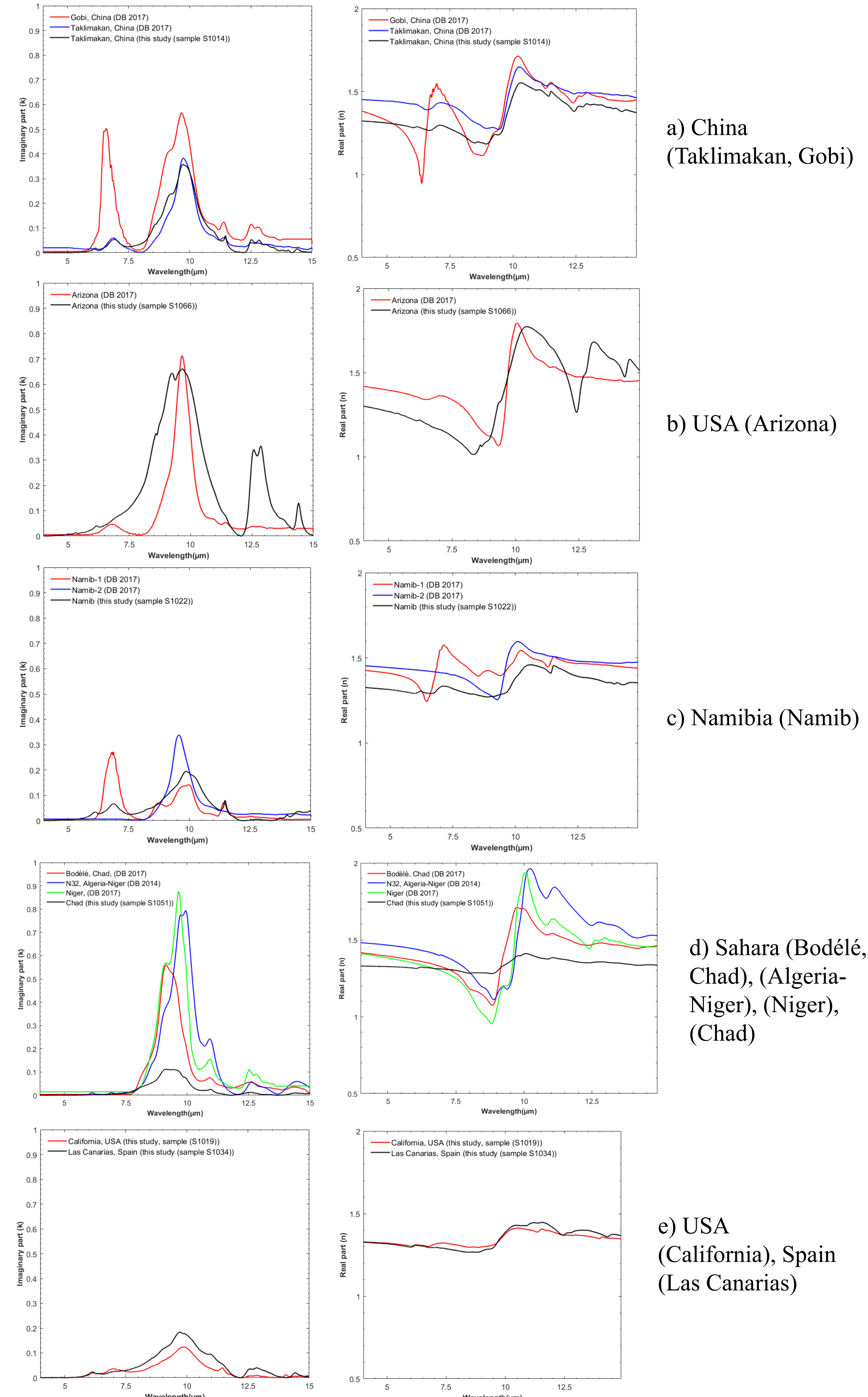


Fig 6. (a-d) Comparison of n and k obtained from this study (in black) with the ones estimated by DB 2014 and DB 2017 for samples from similar/same geographical location. (e) shows the derived n and k for samples (USA and Spain) from this study.

References

Dalton, J. B., and K. M. Pitman (2012), Low temperature optical constants of some hydrated sulfates relevant to planetary surfaces, *Journal of Geophysical Research-Planets*, 117, 15, doi:10.1029/2011je004036.

Di Biagio, C., H. Boucher, S. Caquaque, S. Chevaillier, J. Cuesta, and P. Formenti (2014), Variability of the infrared complex refractive index of African mineral dust: experimental estimation and implications for radiative transfer and satellite remote sensing, *Atmospheric Chemistry and Physics*, 14(20), 11093-11116, doi:10.5194/acp-14-11093-2014.

Di Biagio, C., et al. (2017), Global scale variability of the mineral dust long-wave refractive index: a new dataset of in situ measurements for climate modeling and remote sensing, *Atmospheric Chemistry and Physics*, 17(3), 1901-1929, doi:10.5194/acp-17-1901-2017.

Engelbrecht, J. P., H. Moosmüller, S. Pincock, R. K. M. Jayanty, T. Lersch, and G. Casuccio (2016), Technical note: Mineralogical, chemical, morphological, and optical interrelationships of mineral dust re-suspensions, *Atmospheric Chemistry and Physics*, 16(17), 10809-10830, doi:10.5194/acp-16-10809-2016.

Hale, G. M., and M. R. Querry (1973), Optical Constants of Water in the 200- μm to 200- μm Wavelength Region, *Appl. Opt.*, 12(3), 555-563, doi:10.1364/AO.12.000555.

Roush, T. L. (2021), Estimation of visible, near-, and mid-infrared complex refractive indices of calcite, dolomite, and magnesite, *Icarus*, 354, 13, doi:10.1016/j.icarus.2020.114056.

Sadrian, M. R., Calvin, W. M., Engelbrecht, J. P., Moosmüller, H.: Spectral characterization of parent soils from globally important dust aerosol entrainment regions. Under review in *Journal of Geophysical Research: Atmospheres*.

Salisbury, J. W., L. S. Walter, N. Vergo, and D. M. D'Aría (1991), *Infrared (2.1 - 25 μm) spectra of minerals*, Johns Hopkins University Press, ISBN: 0-8018-4423-1.